European Journal of Medicinal Chemistry 76 (2014) 376–386

Contents lists available at ScienceDirect

European Journal of Medicinal Chemistry

journal homepage: http://www.elsevier.com/locate/ejmech

Original article

Design, synthesis and biological evaluation of D-ring opened galantamine analogs as multifunctional anti-Alzheimer agents

Lei Fang [a,b], Xubin Fang [a], Shaohua Gou [a,*], Amelie Lupp [c], Isabell Lenhardt [c], Yanyan Sun [a], Zhangjian Huang [b], Yao Chen [d], Yihua Zhang [b], Christian Fleck [c,*]

[a] Jiangsu Province Hi-Tech Key Laboratory for Bio-medical Research, Pharmaceutical Research Center, School of Chemistry and Chemical Engineering, Southeast University, Nanjing 211189, PR China
[b] State Key Laboratory of Natural Medicines, China Pharmaceutical University, Nanjing 210009, PR China
[c] Institute of Pharmacology and Toxicology, Friedrich Schiller University Jena, Jena, Germany
[d] Institute of Pharmacy, Friedrich Schiller University Jena, Jena, Germany

ARTICLE INFO

Article history:
Received 13 October 2013
Received in revised form
12 February 2014
Accepted 13 February 2014
Available online 14 February 2014

Keywords:
Anti-Alzheimer
AChE inhibitors
Neuroprotective agents
Aβ aggregation inhibitors
Galantamine analogs

ABSTRACT

Facing the multifactorial nature of Alzheimer's disease, twelve dibenzofuran/carbazole derivatives, which can be considered as the D-ring opened analogs of galantamine, have been designed and synthesized as multifunctional anti-Alzheimer agents. In vitro tests revealed that compounds **3** and **5**, which bear a nitrate moiety in the molecule, showed a potent inhibition activity towards AChE and compound **3** showed a good Aβ42 aggregation inhibitory activity. Moreover, **3** and **5** could also release a relative low concentration of NO in vitro and they did not show toxicity to neuronal cells, while exerted a neuroprotective effect against the Aβ-induced toxicity. More importantly, compound **3** showed a significant spatial memory improving effect in vivo, and a good safety in the ex vivo toxicity study.

1. Introduction

Alzheimer's disease (AD) is the most prominent form of dementia affecting the aged with high incidence. Despite AD has been found for more than 100 years, it is still incurable up to date. The pathophysiology of AD is very complicated. Many studies revealed that AD is a multifactorial syndrome derived from a complex array of neurochemical factors, including the deficiency of synaptic acetylcholine (ACh) and other related neurotransmitters, the formation of neurotoxic β-amyloid peptide (Aβ), oxidative stress, the inflammation of neurons, and so on [1,2]. Thanks to the elucidation of the AD mechanism during the past 2 decades, a variety of etiology hypotheses (e.g. cholinergic hypothesis, amyloid hypothesis, oxidative hypothesis, etc.) have been brought out, leading to various therapeutic strategies. However, only four drugs are clinically available for the treatment of AD so far; they are three acetylcholinesterase inhibitors (AChEIs, including rivastigmine, donepezil and galantamine; the oldest AChEI tacrine was withdrawn from the market due to its serious hepatotoxicity) and one N-methyl-D-aspartic acid (NMDA) receptor antagonist (memantine). The rationale of AChEIs, which were developed based on the cholinergic hypothesis [3,4], is mainly aiming to enhance the levels of synaptic ACh and consequently improve the cholinergic function in the central nervous system. AChEIs can slow the progression of AD and postpone the cognitive deterioration of the patients, acting as the mainstay for the symptomatic treatment of AD. Nevertheless, as mentioned above, AD is a multifactorial disease, and traditional AChEIs like tacrine and donepezil can only hit AChE one target without influence on other pathogenic factors of AD, especially Aβ and its aggregates which play a key role in triggering a neurotoxic cascade and have been considered as a primary target for developing novel anti-AD candidates (e.g. carbazole-based fluorophores [5] and bifunctional metal chelators [6]). Thereby, AChEIs can offer only a palliative effect, but not halt the progression of the disease. Facing the multifactorial nature of AD, researchers have now turned to develop the so called multi-target directed ligands which are able to simultaneously modulate different targets involved in the AD cascade [7]. As the cholinergic and Aβ-related pathways play key roles in the progression of the

* Corresponding authors.
E-mail addresses: sgou@seu.edu.cn (S. Gou), Fleck-Christian@t-online.de (C. Fleck).

http://dx.doi.org/10.1016/j.ejmech.2014.02.035
0223-5234/

disease, they have been considered as the main targets of the multifunctional ligands.

Galantamine (**1**, Fig. 1) is a natural AChEI approved for the treatment of AD in many countries. It has a unique dual mechanism of action, combining allosteric modulation of nicotinic receptors with reversible, competitive inhibition of AChE [8]. Besides, it also exhibits less toxicity than other AChEIs like tacrine. Due to such unique properties, galantamine has been presented as an ideal leading structure for developing multi-target directed ligands. It is noted that much effort has been made in the past decade. The structural modifications of galantamine by previous researches were mostly carried out at the 6-position hydroxyl group and the 11-position nitrogen atom to which a second pharmacophore was incorporated to enhance the anti-AD activity [9–13]. However, such structural modifications usually took galantamine as a starting material, resulting in larger and more complex molecules than galantamine itself, which may possibly cause pharmacokinetic problems. There are also some reports concerning the galantamine analogs whose structural backbone is different from that of galantamine. [14,15] However, the focus of these studies was on the synthetic chemistry, while not on the medicinal chemistry.

Our drug design strategy is to develop novel facile-prepared galantamine analogs by simplifying the backbone of galantamine. From the chemical point of view, galantamine contains two structural units of a universal tricyclic benzofuran core with a sterically congested quaternary carbon and a complex seven-member azepine ring. Notably, the sterical C2 allylic alcohol moiety and the quaternary carbon are very difficult to be constructed via common synthetic procedures. However, according to the classic structure–activity relationship theory of AChEIs, these two fragments are not essential for the activity of galantamine, while the aromatic moiety (i.e. the benzene ring) and the nitrogen atom are. X-ray crystal structure of galantamine bound in the active site of AChE also revealed that the AChE inhibitory activity of galantamine is due to the interaction of the benzene ring with Trp84 via π–π stacking action and the interaction of the nitrogen atom with Asp72 via H-bond action [16]. Therefore, we can hypothesize that the benzofuran fragment and the nitrogen atom are exact pharmacophores responsible for the activity, while the other parts of the molecular structure, including the complex congested quaternary carbon and the seven-membered azepine ring, can be simplified to generate novel facile-prepared galantamine analogs. With this regard in mind, we attempt to use dibenzofuran/carbazole as the basic skeleton instead of the complex tetracyclic structure of galantamine. Furthermore, the seven-membered azepine ring of galantamine is also made broken to generate a flexible aliphatic side chain, on which an additional pharmacophore, such as a nitric oxide (NO) donor (e.g. organic nitrate), can be introduced, leading to novel dibenzofuran/carbazole-NO donor hybrid compounds (Fig. 1). Our design strategy is upon the following factors that i) the designed compounds, which maintain the aromatic moiety and the nitrogen atom, will probably retain or even improve the AChE inhibitory activity of galantamine; ii) the simplified structure of the target molecules makes them possible to be prepared via common synthetic reactions; iii) more importantly, the introduction of the NO-donor moiety, which is able to release NO in vivo, will benefit the anti-AD activity. NO is a key signaling molecule involved in the regulation of many physiological processes. It is also reported that NO plays an important role in the nervous system [17]. Our previous studies indicated that tacrine-NO donor hybrid compounds can enhance the anti-AD activity both in vitro and in vivo [18,19]. Therefore, a synergic action of the dibenzofuran/carbazole scaffold and the NO donor can be expected. In order to predict whether the target compounds retain the AChE inhibitory activity of galantamine we preliminarily performed a simulant study using MOE software. The overlap study of galatamine and the D-ring opened analog showed that the benzofuran ring almost total covers the B and C ring of galantamin; a clear difference between these two molecules is that the tricyclic aromatic system of the analog extends about 7.9 Ang while the partially saturated galantamine tricyclic system is bent over, thus it is 2.5 Ang shorter (Fig. S3, supporting information). Docking compound **2a** to AChE (Protein Data Bank code 3I6M) also revealed that the ligand could effectively enter the enzyme pocket and block the catalytic site of AChE via π-π conjugation and H-bond. These results preliminarily proved our drug design rationale that the simplified molecules could retain the AChE inhibitory activity of galantamine (Fig. S4, supporting information).

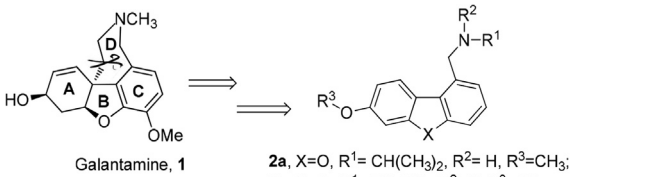

Galantamine, **1**

2a, X=O, R^1= $CH(CH_3)_2$, R^2= H, R^3=CH_3;
2b, X=O, R^1=CH_2CH_3, R^2=H, R^3=CH_3;
2c, X=O, R^1=CH_3, R^2=CH_2CH_3, R^3=CH_3;
2d, X=O, R^1=CH_2CH_3, R^2=CH_2CH_3, R^3=CH_3;
2e, X=O, R^1=CH_2Ph, R^2=H, R^3=CH_3;
2f, X=O, R^1=$CH(CH_3)_2$, R^2=H, R^3=H;
3, X=O, R^1=$CH(CH_3)_2$, R^2=$CO(CH_2)_2ONO_2$, R^3=CH_3;
4a, X=NH, R^1=$CH(CH_3)_2$, R^2= H, R^3=CH_3;
4b, X=NH, R^1=CH_2CH_3, R^2=CH_2CH_3, R^3=CH_3;
4c, X=NH, R^1=CH_2Ph, R^2=H, R^3=CH_3;
4d, X=NH, R^1=$CH(CH_3)_2$, R^2=H, R^3=H;
5, X=NH, R^1=$CH(CH_3)_2$, R^2=$CO(CH_2)_2ONO_2$, R^3=CH_3

Fig. 1. The molecular structures of galantamine (**1**), dibenzofuran derivatives (**2a**–**2f**, **3**) and carbazole derivatives (**4a**–**4d**, **5**).

2. Results and discussion

2.1. Synthesis of the target compounds

For the synthesis of the dibenzofuran derivatives, the previous reported protocol was employed with minor modifications [20]. Generally, 3-bromo-4-nitrophenyl methyl ether reacted with *m*-cresol in the presence of potassium hydroxide to give the nitrodiaryl ether intermediate (**6**), which was further reduced catalytically by hydrogen, forming the amine product (**7**). The cyclization to dibenzofuran was carried out via two steps: firstly treating **7** with $NaNO_2$ under acid condition yielded the diazotized *o*-(ary1oxy) aniline intermediate (**8**); and secondly a mixture of the dibenzofuran derivatives (**9a**, **9b**) was obtained via a free-radical cyclization. The mixture (as judged from ^{1}H NMR spectra and HPLC result the ratio of **9a**:**9b** is about 3:2, see Supporting Information, Fig. S1) can hardly be separated, but after bromination by *N*-bromosuccinimide (NBS) and the treatment of the corresponding amines the products **2a**–**2e** can be successfully obtained (Scheme 1). Compound **2a** was hydrolyzed by treating with 48% HBr aqueous solution, giving the phenol product **2f** (Scheme 3). To introduce the organic nitrate moiety, compound **2a** was acylated by 3-chloropropanoyl chloride to give the chloride intermediate, which was further treated with silver nitrate to give product **3** (Scheme 3).

The synthesis of the carbazole derivatives is different from that of dibenzofurans since the carbazole scaffold can not be constructed via the cyclization reaction due to the NH group of carbazole. Therefore, Suzuki reaction and the modified Cadogan reaction [21] were employed to prepare the carbazole scaffold. In detail, 1-bromo-4-methoxy-2-nitrobenzene was treated with 2-methylphenylboronic acid in the presence of catalytic amount of

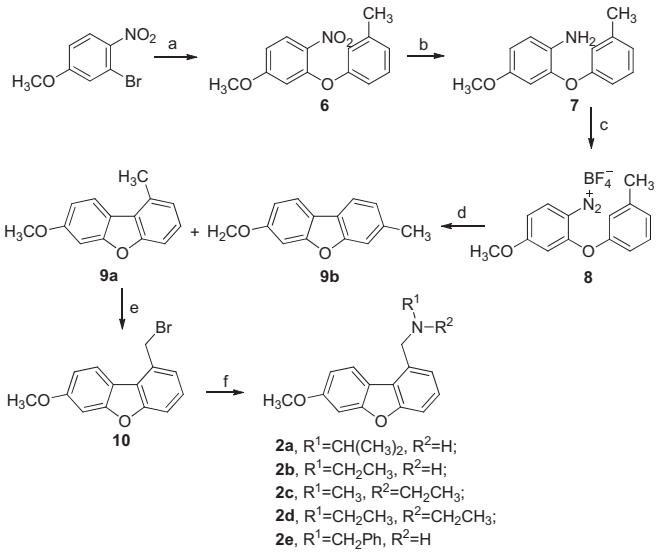

Scheme 1. Synthetic route of dibenzofuran derivatives. Reagents and condition: a) KOH, *m*-cresol, 130 °C → 170 °C, 2 h; b) H_2 (5 Mpa), 10% Pd/C, 50 °C, 5 h; c) 18% HCl, $NaNO_2$, $NaBF_4$, −5 °C, 20 min; d) 1 M H_2SO_4, Cu_2O, 70 °C, 3 h; e) NBS, AIBN, CCl_4, reflux, 3 h; f) alkylamine, KI, anhydrous K_2CO_3, CH_2Cl_2, RT, overnight.

$Pd(PPh_3)_4$ to give the nitrobiphenyl intermediate (**11**). Subsequently, the cyclization of the nitrobiphenyl was achieved via reductive deoxygenation of the nitro group using a slight excess of triphenylphosphine in *o*-dichlorobenzene, resulting in the carbazole compound (**12**). Thereafter, we tried to directly treat **12** with NBS, as we did in the dibenzofuran case, to obtain the benzylic bromination intermediate. However, only the electrophilic aromatic bromination products were obtained after this reaction, which is probably because of the electron donating ability of the NH group of compound **12**. Thus, compound **12** was firstly reacted with benzenesulfonyl chloride to yield the sulfonylated compound **13**, which was then treated with NBS to offer the desired benzylic bromination product (**14**). After treating **14** with corresponding

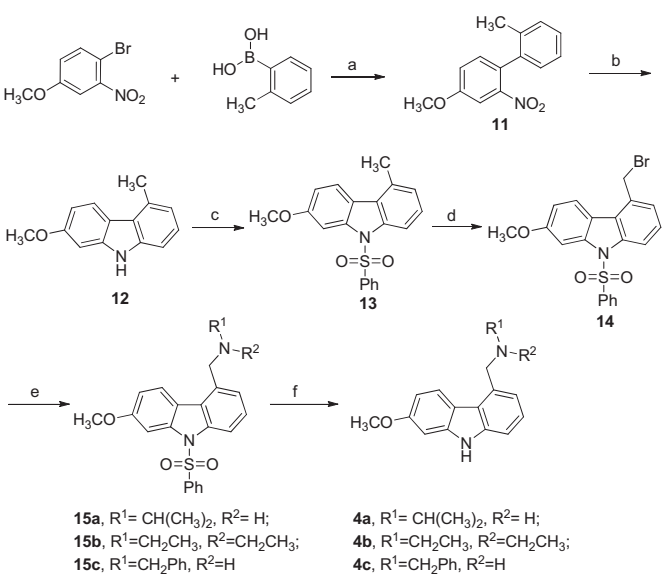

Scheme 2. Synthetic route of carbazole derivatives. Reagents and condition: a) $Pd(PPh_3)_4$, Na_2CO_3, DME, reflux, 20 h; b) PPh_3, DCB, reflux, 3 h; c) $PhSO_2Cl$, NaH, THF, 0 °C → RT, overnight; d) NBS, AIBN, CCl_4, reflux, 3 h; e) alkylamine, KI, K_2CO_3, anhydrous acetone, RT, overnight; f) 2 N NaOH, ethanol, reflux, overnight.

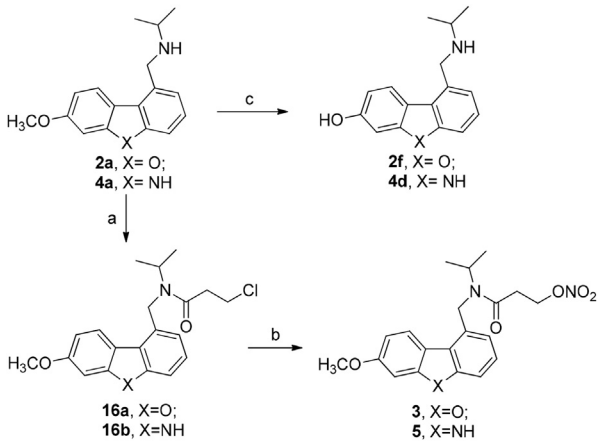

Scheme 3. Synthetic route of NO donor hybrid compounds. Reagents and condition: a) pyridine, CH_2Cl_2, 3-chloropropanoyl chloride, −5 °C, 1 h; b) $AgNO_3$, anhydrous CH_3CN, reflux, 24 h; c) 48% HBr aqueous solution, reflux, 3 h.

amines, compound **15a**–**15c** was obtained, respectively, and then transformed into compound **4a**–**4c** by removing the protecting group (Scheme 2). The synthesis procedure of compound **4d** and **5** was as same as that of compound **2f** and **3**, respectively (Scheme 3).

2.2. Cholinesterase inhibition assay in vitro

The AChE inhibitory activity of the analogs was screened by Ellman's assay in vitro (Table 1). Most of the synthesized compounds showed moderate to potent inhibitory effect on the cholinesterases, except for **2c**, **2e** and **4c** towards AChE. The AChE inhibitory activity of compounds **2a** and **5** is in magnitude at the same order of galantamine, with IC_{50} values in the single to double digit micromole range, while the activity of compound **3** (IC_{50} 0.18 μM) is 60-fold higher than galantamine (IC_{50} 10.53 μM). As far as butyrylcholinesterase (BChE, another cholinesterase isomer responsible for the hydrolysis of ACh) is concerned, all analogs showed higher inhibitory activity than galantamine (Table 1), indicating the analogs can be considered as dual inhibitors towards both AChE and BChE. Analysis of the structure–activity relationship of the synthesized compounds revealed that the activity of dibenzofuran derivatives is generally better than that of carbozole derivatives. The substituents of the nitrogen atom seem have influence on the activity. The alkyl substituents are superior to the aralkyl substituents since **2e** and **4c** only showed a very weak activity. Comparing the activity of **2a** and **4a** with **2e** and **4d**, respectively, we could also found that converting the methyl ether group to phenol group would slightly decrease the inhibition activity. Interestingly, compounds **3** and **5**, which are hybrid compounds derived from compounds **2a** and **4a** connected to a NO donor moiety, showed a significantly improved inhibitory activity. This finding is consistent with our previous result [18,19]. The improved activity is probably due to the introduction of the nitrate group, as our former study indicated that it could interact on the residue Trp279 of the peripheral anionic site of AChE via a hydrophobic action. [19]

2.3. In vitro nitric oxide release assay

Furthermore, in order to investigate the NO-releasing ability of the target compounds, compounds **3** and **5** were selected to perform Griess assay in vitro. It is well known that a nitrate group is able to release NO via either enzymatic or nonenzymatic pathways [22]. Thus, the in vitro nitric oxide release was tested under two

Table 1
Inhibitory effect of **2a**–**2f**, **3**, **4a**–**4d**, **5** and galantamine on AChE and BChE (IC_{50} values).

Compound	IC_{50} (μM) ± S.E.M.[a]		Selectivity ratio[c]
	AChE[b]	BChE[b]	
Galantamine	10.53 ± 3.11	39.03 ± 12.11	0.27
2a	11.60 ± 3.41	13.5 ± 3.1	0.86
2b	18.92 ± 4.08	22.18 ± 7.12	0.85
2c	>>50	Not tested	–
2d	39.11 ± 8.80	27.39 ± 7.76	1.43
2e	>>50	18.1 ± 9.4	–
2f	22.6 ± 7.4	18.36 ± 3.1	1.23
3	0.18 ± 0.04	14.3 ± 3.2	0.13
4a	50.83 ± 12.13	10.08 ± 7.7	5.03
4b	37.91 ± 8.44	14.88 ± 2.08	2.54
4c	>>50	29.9 ± 1.79	–
4d	43.49 ± 5.02	17.27 ± 1.16	3.54
5	2.21 ± 0.51	2.50 ± 0.90	0.88

[a] Data are the means of at least three determinations.
[b] AChE from Electric Eel and BChE from equine serum were used.
[c] Selectivity ratio= (IC_{50} of AChE)/(IC_{50} of BChE).

different conditions: i) incubation of the test compound with only phosphate buffer solution (PBS) at pH 7.4 and 37 °C for 24 h, ii) incubation of the test compound in PBS at pH 7.4 and 37 °C to which 90 μL rat serum had been added. The results (Fig. 2) showed that the %NO released from the nitrate of compounds **3** and **5** in PBS at pH 7.4 varied over a 4.8–6.1% range, which is indicative of a moderate release of NO. The NO release ability of **3** and **5** was slightly improved when the measurement was performed in PBS containing rat serum. This is probably due to that the thiols or enzymes contained in the serum are able to promote the decomposition of the nitrate. Low concentration of NO is essential for the growth of neurons. It was reported that some NO donors or NO mimetic molecules had shown a positive effect on the treatment of AD [17]. Our previous studies also indicated that NO-releasing tacrine derivatives can enhance the anti-AD activity both in vitro and in vivo, probably due to the vasorelaxant effect of NO [18]. In this context, it may be anticipated that the NO release ability of **3** and **5** may present some additional anti-AD properties, though further works need be done to confirm it.

2.4. ThT fluorescence assay

Aβ and its aggregates have been believed to be key etiological factors triggering a neurotoxic cascade and finally causing neurodegeneration in AD brains. In vivo monomeric Aβ42 peptides come from the amyloid precursor protein (APP) cleaved by β- and γ-secretase. The monomeric Aβ42 peptides, spontaneously or bioactivated by various factors, prone to aggregate and subsequently form toxic oligomeric intermediates and plaque-associated amyloid fibrils. Thus, inhibition of the Aβ aggregation has been presented as a promising approach for the development of anti-AD agents. It was reported previously that carbazole and benzofuran scaffolds had ability to inhibit Aβ aggregation [5,23]. In order to investigate the inhibitory effect of the synthesized analogs on Aβ aggregation, compound **3** (5, 50, 100 μM), which showed good activity in all former tests, and galantamine (5, 50, 100 μM) were selected to perform Thioflavin T (ThT) assay. Curcumin was used as positive control. The results are presented in Fig. 3. At a concentration of 5 μM, neither curcumin nor the test compound showed significant inhibitory effect on the aggregation of Aβ42. As the concentration increased, the inhibition rate of curcumin and **3** was enhanced. At a concentration of 50 μM, the inhibition rate of curcumin and **3** reached 24% and 19%, respectively. When the concentration was raised to 100 μM, the inhibition rate of curcumin and **3** was also increased to 29% and 25%, respectively, which is indicative of dosage-dependent manner of the inhibition. As for galantamine, no significant inhibition was observed no matter low or high concentration of galantamine was used. Clearly, in comparison with galantamine compound **3** showed additional anti-Aβ42 aggregation activity, which may alleviate the Aβ-induced toxicity and eventually benefit the treatment of AD.

2.5. Atomic force microscopy

It is well known that a fluorescence intensity-based assay is prone to produce false positives because of fluorescence quenching due to absorbance from colored compounds [24]. Therefore, the formation of Aβ aggregates was visualized using Atomic Force Microscopy (AFM) to confirm the inhibition activity of the target compound. As compared with the blank sample (see Supporting Information Fig. S2, a), the model sample (see Supporting Information Fig. S2, b) without any additive contained high density of typical Aβ amyloid fibrils. In contrast, the sample incubated with compound **3** (50 μM) contained only a number of aggregates,

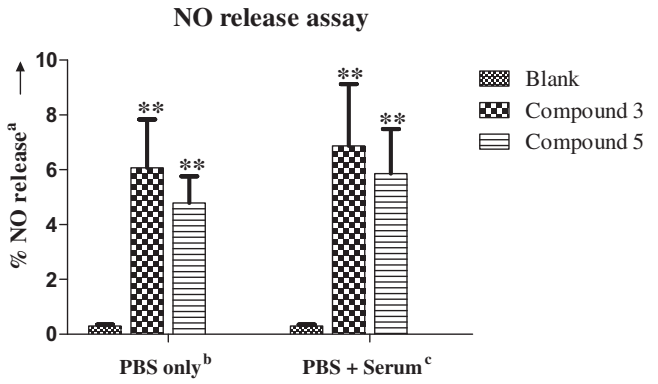

Fig. 2. NO release ability: a) Percent of nitric oxide released based on a theoretical maximum release of 1 mol of NO/mol of the nitrate test compound. The result is the mean value of 3 measurements ($n = 3$) where variation from the mean % value was ≤0.2%. b) A solution of the test compound (2.4 mL of a 100 μM) or solvent vehicle (2.4 mL) in phosphate buffer at pH 7.4 was incubated at 37 °C for 24 h. c) A solution of the test compound (2.4 mL of a 100 μM) or solvent vehicle (2.4 mL) in phosphate buffer at pH 7.4, to which 90 μL rat serum had been added, was incubated at 37 °C for 24 h. Statistical analysis was performed by the one-way ANOVA followed by Tukey's multiple comparison test. $^{**}p < 0.01$ vs. blank.

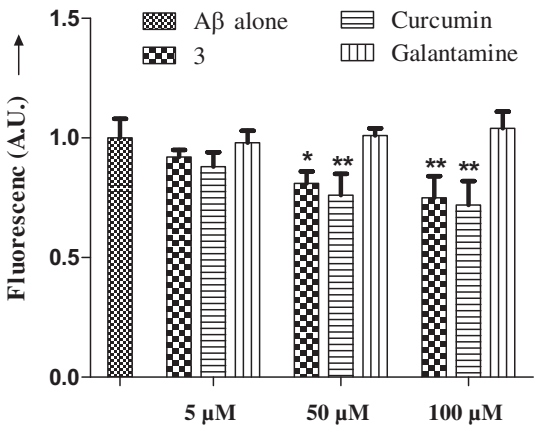

Fig. 3. Inhibition of amyloid formation by compound **3**, curcumin and galantamine monitored by ThT fluorescence. The result is the mean value of 3 measurements ($n = 3$) ± SEM. Statistical analysis was performed by the one-way ANOVA followed by Tukey's multiple comparison test. $^{*}p < 0.05$ vs. Aβ alone, $^{**}p < 0.01$ vs. Aβ alone.

but without fibrils (see Supporting Information Fig. S2, c). According to AFM histogram profile analysis, the sample with compound 3 had the aggregates with the average height of 2.15 nm, while aggregates contained in the control samples had the average height of 8.68 nm. The findings, which are in accordance with the ThT data, apparently indicate a moderate inhibition effect of compound **3**.

2.6. Cell viability analysis

Clinically, most AD patients are diagnosed at the middle to late phase of the disease; that means a great number of Aβ oligomers/fibrils already exist in the patients' brain when the treatment starts. In this context, the agents capable of protecting the neurons from the toxicity of Aβ aggregates seem more attractive than the Aβ aggregation inhibitors. Thus, it will be interesting to investigate whether compound **3**, which already showed Aβ aggregation inhibitory activity in vitro, also possesses neuron protective effect against Aβ-inducing toxicity. By using a previously reported procedure [25] compound **3** was screened for such activity. When PC12 cells were incubated with different concentrations of compound **3** (0.08, 0.4, 2, 10 μM) for 24 h, no cytotoxicity was observed as compared with the vehicle group (control), even at the highest concentration tested (10 μM). In contrast, Aβ42 (5 μM) induced a significant, albeit moderate, toxicity to PC12 cells upon exposure for 24 h as the viability of the cells dropped from 1 to 0.82. Interestingly, when PC12 cells were co-treated with Aβ42 (5 μM) and different concentrations of compound **3** (0.08, 0.4, 2, 10 μM), the toxicity was diminished in a dose-dependent manner, indicating a neuroprotective effect of compound **3**. As for galantamine, the protective effect was not observed (Fig. 4). The neuroprotective effect of **3** is probably due to the NO donor moiety. It was reported that NO released from NO donor like nitrate or furoxans could effectively prevent neurons from the treatment with neurotoxic agents [26,27].

2.7. Behavioral studies in vivo

In vivo study is essential for the pharmacological evaluation of drug candidates, especially for anti-AD substances since many of them met failure previously due to the poor penetration of the blood-brain-barrier and low bioavailability in vivo. In order to determine the in vivo activity of the target compounds, we used

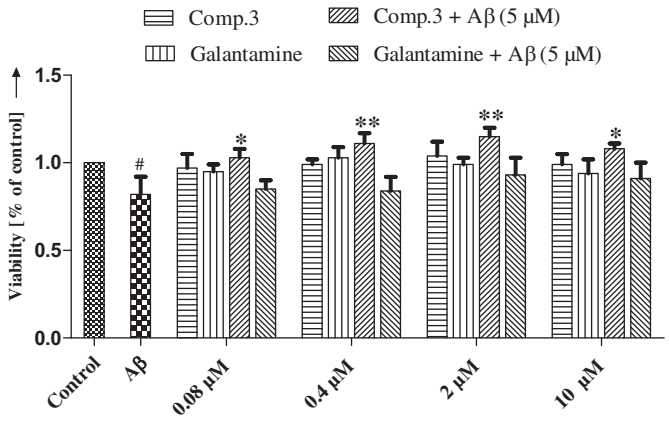

Fig. 4. Neuroprotective effects of tested compounds against Aβ42-induced cytotoxicity towards PC12 cells. The result is the mean value of 3 measurements ($n = 3$). Data were subjected to one-way ANOVA followed by Dunnett's multiple comparison post-test. $^{*}p < 0.01$ vs. Aβ group, $^{**}p < 0.001$ vs. Aβ group, $\#p < 0.05$ vs. control group.

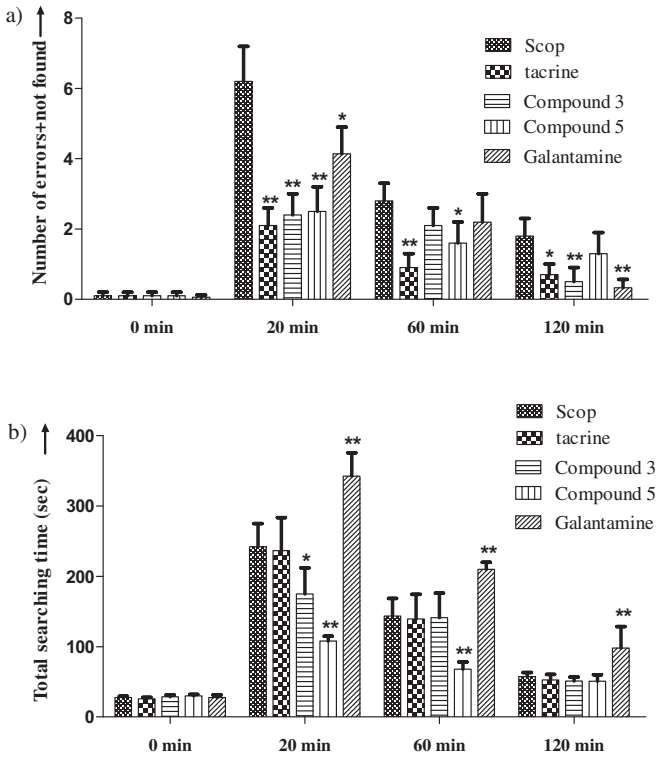

Fig. 5. Influence of tacrine, galantamine, compounds **3** and **5** (each 1 μmol/100 g b. wt.) on scopolamine (0.05 mg/100 g b. wt.) induced impairment of working memory in adult rats measured in an eight-arm radial maze. The result is the mean value of 14 measurements ($n = 14$) ± SEM. a) Errors made plus baits not found after 10 min. b) Total searching time. Statistical analysis was performed by the one-way ANOVA followed by Tukey's multiple comparison test. $^{*}p < 0.01$ vs. scop group, $^{**}p < 0.001$ vs. scop group.

cognition impaired adult rats (after scopolamine [scop] administration) as animal model to measure the cognition improving effects of compounds **3** and **5**. Galantamine and tacrine were chosen as positive control, respectively. The measurement was performed in an eight-arm radial maze, which is an accepted tool in behavioral pharmacology [28]. After the rats were adapted to the maze and trained to be able to quickly find the bait at the end of each arm, they were treated with scopolamine (0.05 mg/100 g b. wt., i.p.). Scopolamine distinctly blocks muscarinic cholinergic receptors, and thus caused reversible impairment of the animals' cognition. Then tacrine (1 μmol/100 g b. wt.) as well as compounds **3**, **5**, and galantamine (equimolar dose), which are supposed to more or less compensate for the cholinergic dysfunction in the central nervous system by inhibiting AChE, were administered to the animals, respectively. Two behavioral parameters, i.e. the total searching time for all baits and the sum of the number of errors made during the exploration plus the number of the baits not found after 10 min (errors plus baits not found), were recorded 0, 20, 60, and 120 min after scopolamine administration to determine the cognition improving activity of the selected compounds. Given the scopolamine-induced cognition impairment usually fades within 2 h, the data obtained at 20 min are more valuable for discussion.

The results are shown in Fig. 5. At 20 min, the amount of errors plus baits not found of the model group (i.e. scop group) increased from 0 at 0 min to 6.2, and the total exploration time also increased from 28 to 242 s, indicating an obvious impairment of working memory and animals' behavior caused by scopolamine. When the animals were co-treated with tacrine, compounds **3** or **5**, the amount of errors plus baits not found significantly decreased to 2.1,

2.4, 2.5, respectively (Fig. 5, a). Besides, the total exploration time of the compound **3** and **5** group also decreased from 242 s to 175 and 107 s, respectively, while the searching time of the tacrine group (237 s) was not shortened (Fig. 5, b). For both errors plus baits not found and the searching time parameters, statistically significant differences can be observed between the scop group and the compounds **3** and **5** groups, respectively. Apparently, both compounds **3** and **5** effectively alleviated the cognitive deficits induced by scopolamine. The activity of galantamine was not as good as the other test compounds in the assay. This is probably because of its relative low AChE inhibitory activity.

In order to more comprehensively evaluate the activity of the test compounds, we developed a scoring system, which considers both the exploration time and errors plus baits not found, to quantify the performance of the rats in the assay. The calculation of the score is based on the following equation: Score = errors plus baits not found + total exploration time (seconds)/100. The lower the score is, the better the performance of the rats is. Table 2 shows the scores of the tacrine, galantamine, compound 3 and 5 groups, respectively. The lowest scores of compound **3** and **5** groups suggest the best performance of the corresponding rats in the assay. The tacrine and galantamine groups got higher scores, which attribute to the long searching time needed to find all food baits. Notably, it was observed that the treatment with tacrine, no matter with or without scopolamine, likely caused a significant slow-down of the rats' movement in the maze, which may result from the tacrine-related cholinergic events, whereas the treatment with compounds **3** and **5** had no influence on the rats' movement at all. These findings indicate that, in addition to the better spatial memory improving effect in vivo, the target compounds **3** and **5** also possess advantages in terms of safety in comparison to tacrine.

2.8. Biochemical investigations ex vivo

For more precise information about the safety of the target compounds, we further applied an ex vivo study to investigate the toxicity of compound **3** towards liver, kidney and brain tissues, using tacrine as a reference control. After treatment with tacrine (1 or 6 μmol/100 g b. wt.) or equimolar doses of the novel compound **3** for 24 h, respectively, the rats were killed and the corresponding tissues were separated. Five parameters, including levels of reduced glutathione (GSH), oxidized glutathione (GSSG), total glutathione, lipidperoxidation products (LPO), and the weight of the organ, were measured and recorded. For a more comprehensive study of hepatotoxicity, which is one of the serious side effects of tacrine, additional data of protein content, activity of ethylmorphine *N*-demethylation (END), ethoxycoumarin *O*-deethylation (EcOD) and ethoxyresorufin *O*-deethylation (ErOD) were also collected (see Supporting Information, Table S1).

It was found that the treatment with the highest tolerated dose (6 μmol/100 g b. wt.) of tacrine led to severe toxicity towards liver tissue as indicated by the significantly decreased liver weight, reduced GSH and total glutathione content, and diminished END and EcOD activity. In contrast, no statistically significant difference was observed between the compound **3** group and the control group, hinting no hepatotoxicity was caused by compound **3** at all. As for brain and kidney tissues, both tacrine and compound **3** induced an increased ratio of GSH/GSSG and a lower level of lipidperoxidation products, suggesting no oxidative damage caused by them.

Table 2
Scores of tacrine, galantamine, compound **3** and **5** groups.

Time after scop treatment (min)	Score[a]				
	Scop	Tacrine	3	5	1
20	8.6	4.5	3.7	3.1	7.4
60	4.3	2.3	3.5	1.9	4.3
120	2.4	1.2	1.0	1.8	1.3

[a] Score = errors plus baits not found + total searching time (seconds)/100.

3. Conclusion

Due to the multifactorial nature of AD the multi-target directed agents hold considerable promise as a therapeutic strategy to combat this incurable disease. Hereby we have designed and synthesized novel dibenzofuran/carbazole derivatives as multifunctional anti-AD agents by means of simplifying the skeleton of the galantamine molecule. In comparison with galantamine, the analogs, especially compound **3**, showed an improved anti-AD activity, combining the cholinesterase inhibition and anti-Aβ aggregation ability. Compounds **3** and **5**, which bear a nitrate moiety in the molecule, could also release a relative low concentration of NO in vitro. Furthermore, in vitro assay revealed that the analogs did not show toxicity to neuronal cells, and could exert a neuroprotective effect against the Aβ oligomer-induced toxicity. More importantly, compound **3** showed a significant spatial memory improving effect in vivo, and the ex vivo toxicity study indicated that no obvious toxicity was caused by compound **3**, suggesting a good safety. Altogether, the results suggest that the dibenzofuran/carbazole derivatives, in particular compound **3**, can be considered as potential therapeutic agents for AD. The work also presents new leading structures for developing novel anti-AD drugs.

4. Experimental protocols

4.1. Chemistry

4.1.1. Materials and instruments

All chemicals and reagents were of analytical reagent grade and were used without further purification. All the solvents were dried by the standard methods wherever needed. IR spectra were measured on KBr pellets with a Nicolet IR200 FTIR spectrometer in the range from 4000 to 400 cm^{-1}. ^1H NMR and ^{13}C NMR were recorded using a Bruker 300/500 MHz spectrometer and referenced to the residue $CHCl_3$ 7.26 ppm or DMSO-d6 2.5 ppm. Low resolution and High resolution mass spectrum measurements were carried out by using Angilent technologies LC/MS TOF. The Purity of the tested compounds was >95% based on the HPLC analysis (Angilent 1260 consisting of G1312C Bin Pump and 1315D DAD UV detector and the mobile phase is water:methanl = 60:40, and the detection wavelength was set at 210 nm). Retention times (t_R) are given in minutes.

4.1.2. Synthesis of 4-methoxy-2-(3-methylphenoxy)-1-nitrobenzene (**6**)

A mixture of *m*-cresol (1.62 g, 15 mmol) and potassium hydroxide (0.84 g, 15 mmol) was heated to 120 °C and stirred for 0.5 h, and then 3-bromo-4-nitrophenyl methyl ether (2.31 g, 10.0 mmol) and copper powder (0.1 g) were added, respectively. The resulting mixture was stirred at 170 °C for 2 h. After cooling down to room temperature, ethyl acetate (50 mL) was added to the reaction mixture. The deposit was filtrated off, and the filtrate was dried with anhydrous Na_2SO_4, and the solvent was removed under vacuum to give the crude product which was furtehr purified by column chromatography (petro ether/EtOAc = 15:1) to give the desired product **6** (1.86 g) in 72% yield as a yellow oil. IR (KBr, cm^{-1}): 3033, 1580, 1513, 1442, 1342, 1290. ^1H NMR (300 MHz, DMSO-d_6): δ 2.31 (s, 3H), 3.81 (s, 3H), 6.59 (d, J = 2.5 Hz, 1H), 6.86

(d, J = 8.0 Hz, 1H), 6.89 (s, 1H), 6.96 (dd, J = 9.0 Hz, 2.5 Hz, 1H), 7.02 (d, J = 8.0 Hz, 1H), 7.32 (t, J = 8.0 Hz, 1H), 8.15 (d, J = 9.0 Hz, 1H). MS(ESI) m/z Calcd for $C_{14}H_{14}NO_4$ $[M + H]^+$ 260.1 found 260.0.

4.1.3. Synthesis of 4-methoxy-2-(3-methylphenoxy)phenylamine (**7**)

Compound 6 (2.6 g, 10.0 mmol) was dissolved in 500 mL of anhydrous ethanol; 5% palladium on charcoal (0.05 g) was added to the solution and the reduction was carried out with hydrogen at an initial pressure of 3 Mpa. After 3 h no more hydrogen was consumed; the catalyst was filtered off and the solvent was removed under vacuum. The obtained crude product was purified by column chromatography (petro ether/EtOAc = 5:1) to give the desired product 7 (2.0 g) in 87% yield as a yellow oil. IR (KBr, cm^{-1}): 3449, 3365, 1583, 1511, 1444, 1156, 1037. ^{1}H NMR (300 MHz, DMSO-d_6): δ 2.26 (s, 3H), 3.60 (s, 3H), 4.41 (s, 2H), 6.41 (d, J = 2.5 Hz, 1H), 6.60 (dd, J = 9.0 Hz, 2.5 Hz, 1H), 6.66–6.76 (m, 3H), 6.87 (d, J = 7.5 Hz, 1H), 7.22 (t, J = 9.0 Hz, 7.5 Hz, 1H). MS(ESI) m/z Calcd for $C_{14}H_{16}NO_2$ $[M + H]^+$ 230.1 found 230.1.

4.1.4. Synthesis of 7-methoxy-1-methyldibenzo[b,d]furan (**9a**) and 3-methoxy-7-methyldibenzo [b,d]furan (**9b**)

To a solution of compound **7** (15.7 g, 68.5 mmol) in 50 mL of 6 mol/L HCl aqueous solution which was cooled to 0 °C, a solution of $NaNO_2$ (5.7 g, 82.3 mmol) in 10 mL of water was added dropwise, keeping the temperature of the reaction mixture not beyond 5 °C. Then the reaction mixture was stirred at 0 °C for another 30 min. The deposit was filtrated off, and the filtrate was treated with sodium tetrafluoroborate (9.0 g, 82.2 mmol) to form white deposit which was collected and added to a mixture of cuprous oxide (11.8 g, 82.2 mmol) in 200 mL of 1 mol/L H_2SO_4 aqueous solution. The resulting mixture was stirred at 60 °C for 2 h. After cooling the reaction mixture to room temperature, the deposit was filtrated off and the filtrate was extracted with AcOEt (100 mL × 3). The organic phase was dried with anhydrous Na_2SO_4, and the solvent was removed under vacuum to give the crude product which was furtehr purified by column chromatography (petro ether/EtOAc = 30:1) to give the mixture of **9a** and **9b** (9a:9b = 3:2). For **9a**, ^{1}H NMR (500 MHz, DMSO-d_6): δ 2.72 (s, 3H), 3.87 (s, 3H), 7.03 (dd, J = 8.5 Hz, 2.5 Hz, 1H), 7.15 (d, J = 7.5 Hz, 1H), 7.31 (d, J = 2.5 Hz, 1H), 7.32 (t, J = 7.5 Hz, 7.5 Hz, 1H), 7.46 (d, J = 7.5 Hz, 1H), 7.97 (d, J = 8.5 Hz, 1H). MS(ESI) m/z Calcd for $C_{14}H_{13}O_2$ $[M + H]^+$ 212.1 found 212.2. For **9b**, ^{1}H NMR (500 MHz, DMSO-d_6): δ 2.46 (s, 3H), 3.86 (s, 3H), 6.98 (dd, J = 8.5 Hz, 2.5 Hz, 1H), 7.18 (d, J = 8.0 Hz, 1H), 7.27 (d, J = 2.5 Hz, 1H), 7.45 (s, 1H), 7.89 (d, J = 8.0 Hz, 1H), 7.94 (d, J = 8.5 Hz, 1H). MS(ESI) m/z Calcd for $C_{14}H_{13}O_2$ $[M + H]^+$ 212.1 found 212.2.

4.1.5. General procedure for the synthesis of **2a–2e**

To the mixture of **9a** and **9b** (0.5 g, 2.4 mmol) dissovled in 30 mL of carbon tetrachloride were added *N*-bromosuccinimide (0.45 g, 2.5 mmol) and azobisisobutyronitrile (0.25 g, 1.5 mmol). The resulting mixture was stirred and refluxed for 3 h. After cooling to room temperature, the deposit was filtrated off and the filtrate was concentrated to give a yellow oil which was then dissolved in 20 mL of CH_2Cl_2. To the obtained solution corresponding amines (20 mmol), potassium carbonate (0.70 g, 5 mmol) and catalytic amount of potassium iodide were added and the reaction mixture was stirred at room temperature for 3 h. The deposit was filtered off and the solvent was removed under vacuum. The obtained crude product was purified by column chromatography (petro ether/EtOAc = 5:1) to give the desired product.

Analytical data for ***N*-((7-methoxydibenzo[b,d]furan-1-yl) methyl)propan-2-amine** (**2a**): yellow oil. Yield 56%. IR (KBr, cm^{-1}): 2958, 1632, 1584, 1437, 1282. ^{1}H NMR (300 MHz, DMSO-d_6): δ 1.18 (d, J = 8.0 Hz, 6H, CH(CH_3)$_2$), 3.02–3.04 (m, 1H, CH(CH$_3$)$_2$), 3.90 (s, 3H, OCH_3), 4.24 (s, 2H, CH_2NCH), 6.97 (dd, J = 8.0 Hz, 2.5 Hz, 1H, arom), 7.11 (d, J = 2.5 Hz, 1H, arom), 7.25 (d, J = 7.5 Hz, 1H, arom), 7.34 (t, J = 8.0 Hz, 7.5 Hz, 1H, arom), 7.44 (d, J = 8.0 Hz, 1H, arom), 7.90 (d, J = 8.0 Hz, 1H, arom). HPLC purity: t_R = 7.56, 98.67%. HRMS (ESI) m/z Calcd for $C_{17}H_{20}NO_2$ $[M + H]^+$ 270.1494 found 270.1488. Anal. Calcd. for $C_{17}H_{19}NO_2$: C, 75.81; H, 7.11; N, 5.20. Found C, 75.76; H, 7.05; N, 5.35.

Analytical data for ***N*-((7-methoxydibenzo[b,d]furan-1-yl) methyl)ethanamine (2b)**: yellow oil. Yield 44%. IR (KBr, cm^{-1}): 3190, 1627, 1511, 1445, 1270. ^{1}H NMR (300 MHz, $CDCl_3$): δ 1.07 (t, J = 7.5 Hz, 3H), 2.59 (q, J = 7.5 Hz, 2H), 3.91 (s, 3H), 4.39 (s, 2H), 6.97 (dd, J = 7.5 Hz, 3.0 Hz, 1H), 7.11 (d, J = 3.0 Hz, 1H), 7.27–7.26 (d, J = 7.5 Hz, 1H), 7.34 (t, J = 7.5 Hz, 1H), 7.45 (d, J = 7.5 Hz, 1H), 7.89 (d, J = 7.5 Hz, 1H). HPLC purity: t_R = 7.69, 99.09%. HRMS (ESI) m/z Calcd for $C_{16}H_{18}NO_2$ $[M + H]^+$ 256.1337 found 256.1342.

Analytical data for ***N*-((7-methoxydibenzo[b,d]furan-1-yl) methyl)-*N*-methylethanamine (2c)**: yellow oil. Yield 41%. IR (KBr, cm^{-1}): 3132, 1631, 1510, 1456, 1270. ^{1}H NMR (500 MHz, $CDCl_3$): δ 1.13 (t, J = 8.00 Hz, 3H), 2.25 (s, 3H), 2.56–2.58 (m, 2H), 3.89 (s, 3H), 3.99 (s, 2H), 6.94 (dd, J = 7.5 Hz, 1.5 Hz, 1H), 7.07 (d, J = 1.5 Hz, 1H), 7.23 (d, J = 7.5 Hz, 1H), 7.29 (t, J = 7.5 Hz, 1H), 7.42 (d, J = 7.5 Hz, 1H), 8.00 (d, J = 7.5 Hz, 1H). HPLC purity: t_R = 8.69, 100%. HRMS (ESI) m/z Calcd for $C_{17}H_{20}NO_2$ $[M + H]^+$ 270.1494 found 270.1489.

Analytical data for ***N*-ethyl-*N*-((7-methoxydibenzo[b,d]furan-1-yl)methyl)ethanamine (2d)**: yellow oil. Yield 67%. IR (KBr, cm^{-1}): 3089, 1632, 1583, 1437, 1280. ^{1}H NMR (300 MHz, $CDCl_3$): δ 0.97 (t, J = 8.00 Hz, 6H), 2.66 (q, J = 7.5 Hz, 4H), 3.91 (s, 3H), 4.04 (s, 2H), 6.94 (dd, J = 7.5 Hz, 3.0 Hz, 1H), 7.09 (d, J = 3.0 Hz, 1H), 7.28 (d, J = 7.5 Hz, 1H), 7.34 (t, J = 7.5 Hz, 1H), 7.91 (d, J = 3.0 Hz, 1H), 8.04 (d, J = 7.5 Hz, 1H). HPLC purity: t_R = 11.60, 98.91%. HRMS (ESI) m/z Calcd for $C_{18}H_{22}NO_2$ $[M + H]^+$ 284.1651 found 284.1656.

Analytical data for ***N*-benzyl-1-(7-methoxydibenzo[b,d]furan-1-yl)methanamine (2e)**: yellow oil. Yield 66%. IR (KBr, cm^{-1}): 3026, 1632, 1584, 1503, 1437, 1279. ^{1}H NMR (500 MHz, $CDCl_3$): δ 3.89 (s, 3H), 3.93 (s, 2H), 4.23 (s, 2H), 6.88 (dd, J = 7.5 Hz, 2.5 Hz, 1H), 7.08 (d, J = 2.5 Hz, 1H), 7.28–7.26 (m, 2H), 7.34–7.31 (m, 3H), 7.37–7.35 (m, 2H), 7.43–7.42 (m, 1H), 7.71 (d, J = 7.5 Hz, 1H). HPLC purity: t_R = 9.80, 100%. HRMS (ESI) m/z Calcd for $C_{21}H_{20}NO_2$ $[M + H]^+$ 318.1494 found 318.1498.

4.1.6. Synthesis of 4-methoxy-2′-methyl-2-nitro-1,1′-biphenyl (**11**)

To a solution of 1-bromo-4-methoxy-2-nitrobenzene (1.2 g, 5.0 mmol) in 15 mL of glycol dimethyl ether was added a solution of palladium-tetrakis(triphenylphosphine) (0.3 g, 0.25 mmol) in 15 mL of glycol dimethyl ether. The resulting mixture was stirred for 15 min at room temperature in a nitrogen atmosphere. Then 2-methylphenylboronic acid (0.95 g, 7.0 mmol) and 20 mL of 2 N Na_2CO_3 aqueous solution were added, respectively. The reaction mixture was stirred and refluxed for 20 h. After cooling the reaction mixture to room temperature, the organic phase was separated and concentrated and finally purified by column chromatography (petro ether/EtOAc = 20:1) to give the desired product **11** (1.20 g) in 98% yield as a yellow solid, m.p. 56–58 °C. IR (KBr, cm^{-1}): 3100, 3010, 2977, 1621, 1536, 1480, 1455, 1356, 1294, 1228, 1119, 1083, 874, 812, 793, 768, 734, 568. ^{1}H NMR (300 MHz, $CDCl_3$): δ 2.09 (s, 3H), 3.92 (s, 3H), 7.08 (dd, J = 7.5 Hz, 1.5 Hz, 1H), 7.18 (dd, J = 8.5 Hz, 2.5 Hz, 1H), 7.23–7.29 (m, 2H), 7.18–7.22 (m, 2H), 7.51 (d, J = 2.5 Hz, 1H). MS(FAB) m/z Calcd for $C_{14}H_{13}NO_3$ $[M]^+$ 243.1 found 243.2.

4.1.7. Synthesis of 2-methoxy-5-methyl-9H-carbazole (**12**)

The solution of compound **11** (2.4 g, 10.0 mmol) and triphenylphosphine (6.6 g, 25.0 mmol) in 50 mL of 1,2-dichlorobenzene was stirred at 180 °C in a nitrogen atmosphere for 3 h. Then the reaction solution was cooled to 35 °C and the solvent was removed under

reduced pressure. The obtained crude product was purified by column chromatography (petro ether/EtOAc = 3:1) to give the desired product **12** (1.80 g) in 85.3% yield as a yellow crystal. m.p. 120–122 °C. IR (KBr, cm^{-1}): 3401, 3053, 2951, 1624, 1607, 1572, 1496, 1306, 1228, 1197, 1119, 819, 754, 725. ^1H NMR (300 MHz, DMSO-d_6): δ 2.74 (s, 3H), 3.85 (s, 3H), 6.81 (dd, J = 8.0 Hz, 2.1 Hz, 1H), 6.91 (d, J = 7.2 Hz, 1H), 6.99 (d, J = 2.1 Hz, 1H), 7.21 (t, J = 7.2 Hz, 1H), 7.28 (d, J = 7.2 Hz, 1H), 7.97 (d, J = 8.0 Hz, 1H), 11.14 (s, 1H). MS(ESI) m/z Calcd for $C_{14}H_{14}NO$ $[M + H]^+$ 212.1 found 213.2.

4.1.8. Synthesis of 2-methoxy-5-methyl-9-(phenylsulfonyl)-9H-carbazole (**13**)

To a solution of sodium hydride (1.2 g, 50.0 mmol) in 50 mL of anhydrous THF which was cooled to 5 °C was added dropwise a solution of compound **12** (2.11 g, 10.0 mmol) in 10 mL of anhydrous THF. The resulting solution was stirred at 5 °C for 1 h. Benzene sulfochloride (2.1 g, 12.0 mmol) was then added dropwise to the reaction solution, controlling the reaction temperature not beyond 5 °C. The reaction solution was stirred over night at room temperature and then poured into 300 mL of cooled water, forming white deposit which was collected via filtration and recrystallized from ethanol to give the desired product **13** (3.23 g) in 92% yield as a light yellow crystal, m.p. 177–179 °C. IR (KBr, cm^{-1}): 3435, 2981, 1621, 1585, 1502, 1479, 1413, 1365, 1287, 1179, 1149, 986, 849, 780, 756, 599. ^1H NMR (500 MHz, DMSO-d_6): δ 2.67 (s, 3H), 3.92 (s, 3H), 7.09 (dd, J = 8.7 Hz, 2.4 Hz, 1H), 7.20 (d, J = 7.5 Hz, 1H), 7.40 (t, J = 8.1 Hz, 7.8 Hz, 1H), 7.53 (t, J = 8.1 Hz, 7.5 Hz, 2H), 7.66 (t, J = 7.8 Hz, 7.2 Hz, 1H), 7.83–7.86 (m, 3H), 8.00 (d, J = 8.7 Hz, 1H), 8.10 (d, J = 8.7 Hz, 1H). MS(ESI) m/z Calcd for $C_{20}H_{18}NO_3S$ $[M + H]^+$ 352.1 found 352.1.

4.1.9. Synthesis of 5-(bromomethyl)-2-methoxy-9-(phenylsulfonyl)-9H-carbazole (**14**)

A solution of **9b** (3.5 g, 10 mmol), *N*-bromosuccinimide (1.98 g, 11.0 mmol), catalystic amount of azobisisobutyronitrile in 30 mL of carbon tetrachloride were stirred and refluxed for 2 h. After cooling to room temperature, the deposit was filtrated off and the filtrate was concentrated to give a yellow oil which was further purified by column chromatography (petro ether/EtOAc = 5:1) to give the desired product **14** (4.09 g) in 95.0% yield as a yellow solid. m.p. 116–118 °C. IR (KBr, cm^{-1}): 3445, 2999, 1619, 1498, 1444, 1290, 1178, 1152, 856, 759, 721, 683. ^1H NMR (300 MHz, DMSO-d_6): δ 3.95 (s, 3H), 5.14 (s, 2H), 7.16 (dd, J = 8.7 Hz, 2.4 Hz, 1H), 7.47 (d, J = 8.1 Hz, 2H), 7.55 (t, J = 8.1 Hz, 7.5 Hz, 2H), 7.65 (d, J = 7.5 Hz, 1H), 7.85 (d, J = 2.4 Hz, 1H), 7.88 (d, J = 1.5 Hz, 1H), 7.92–7.90 (m, 1H), 8.11 (d, J = 8.7 Hz, 1H), 8.24–8.26 (m, 1H). MS(ESI) m/z Calcd for $C_{20}H_{17}BrNO_3S$ $[M + H]^+$ 430.0 found 430.0.

4.1.10. General procedure for the synthesis of **15a–15c**

To a mixture of corresponding amines (25.0 mmol), potassium carbonate (0.70 g, 5.0 mmol) and catalytic amount of potassium iodide in 30 mL of anhydrous acetone was added dropwise a solution of **14** (1.07 g, 2.5 mmol) in 10 mL of anhydrous acetone. The resulting mixture was stirred over night at room temperature. The deposit was filtered off and the filtrate was concentrated under reduced pressure. The obtained crude product was purified by column chromatography (petro ether/EtOAc = 5:1) to give the desired product.

Analytical data for ***N*-((7-methoxy-9-(phenylsulfonyl)-*9H*-carbazol-4-yl)methyl)propan-2-amine** (**15a**): yellow solid, m.p. 111–112 °C. Yield 55%. IR (KBr, cm^{-1}): 3440, 2950, 1630, 1581, 1437, 1282, 1117, 1098, 855, 759, 688. ^1H NMR (300 MHz, $CDCl_3$): δ 1.11 (d, J = 6.3 Hz, 6H), 2.90–2.93 (m, 1H), 3.94 (s, 3H), 4.19 (s, 2H), 7.06 (dd, J = 8.5 Hz, 2.5 Hz, 1H), 7.37 (d, J = 8.0 Hz, 2H), 7.58 (t, J = 8.0 Hz, 7.5 Hz, 2H), 7.66 (d, J = 7.5 Hz, 1H), 7.88 (d, J = 2.5 Hz, 1H), 7.91 (d, J = 1.5 Hz, 1H), 7.92–7.94 (m, 1H), 8.10 (d, J = 8.5 Hz, 1H), 8.20–8.22 (m, 1H). MS(ESI) m/z Calcd for $C_{23}H_{24}N_2O_3SNa$ $[M + Na]^+$ 431.1 found 431.2.

Analytical data for ***N*-ethyl-*N*-((7-methoxy-9-(phenylsulfonyl)-*9H*-carbazol-4- yl)methyl)ethanamine (15b)**: yellow solid, m.p. 90–92 °C. Yield 61%. IR (KBr, cm^{-1}): 3018, 2931, 1625, 1580, 1415, 1280, 1117, 855, 756, 679. ^1H NMR (300 MHz, $CDCl_3$): δ 1.05 (t, J = 7.0 Hz, 6H), 2.58 (d, J = 7.0 Hz, 4H), 3.97 (s, 3H), 4.21 (s, 2H), 7.10 (dd, J = 8.5 Hz, 2.5 Hz, 1H), 7.31 (d, J = 8.0 Hz, 2H), 7.55 (t, J = 8.0 Hz, 7.5 Hz, 2H), 7.69 (d, J = 7.5 Hz, 1H), 7.81 (d, J = 2.5 Hz, 1H), 7.90 (d, J = 1.5 Hz, 1H), 7.92–7.94 (m, 1H), 8.04 (d, J = 8.5 Hz, 1H), 8.18–8.20 (m, 1H). MS(ESI) m/z Calcd for $C_{24}H_{27}N_2O_3S$ $[M + H]^+$ 423.2 found 423.2.

Analytical data for ***N*-benzyl-1-(7-methoxy-9-(phenylsulfonyl)-*9H*-carbazol-4-yl)methanamine (15c)**: yellow solid, m.p. 121–122 °C. Yield 65%. IR (KBr, cm^{-1}): 3412, 2981, 1610, 1481, 1321, 1219, 1190, 947, 775, 760, 730, 696. ^1H NMR (300 MHz, $CDCl_3$): δ 3.85 (s, 3H), 3.88 (s, 2H), 4.18 (s, 2H), 6.86–6.92 (m, 4H), 7.27–7.29 (m, 3H), 7.41 (d, J = 7.2 Hz, 2H), 7.49–7.55 (m, 3H), 7.75–7.77 (m, 2H), 8.25–8.30 (m, 2H). MS(ESI) m/z Calcd for $C_{27}H_{25}N_2O_3S$ $[M + H]^+$ 457.2 found 457.2.

4.1.11. General procedure for the synthesis of **4a–4c**

A solution of compound **15** (2.5 mmol), 10 mL of 2 N NaOH aqueous solution and 40 mL of ethanol was refluxed over night, and then ethanol was removed under reduced pressure. The formed yellow deposit was collected and recrystallized from ethanol to give the desired product.

Analytical data for ***N*-((7-methoxy-*9H*-carbazol-4-yl)methyl) propan-2-amine** (**4a**): yellow solid, m.p. 71–72 °C. Yield 85%. IR (KBr, cm^{-1}): 3295, 2967, 1626, 1610, 1582, 1375, 1236, 1172, 874, 806, 750, 726. ^1H NMR (300 MHz, DMSO-d_6): δ 1.10 (d, J = 6.5 Hz, 6H, CH(CH_3)), 2.92–2.94 (m, 1H, CH(CH_3)$_2$), 3.84 (s, 3H, OCH_3), 4.19 (s, 2H, CH_2NCH), 6.80 (dd, J = 8.6 Hz, 2.5 Hz, 1H, arom), 6.97 (d, J = 2.5 Hz, 1H, arom), 7.11 (d, J = 7.5 Hz, 1H, arom), 7.22–7.24 (m, 1H, arom), 7.31 (d, J = 7.5 Hz, 1H, arom), 7.98 (d, J = 8.6 Hz, 1H, arom), 11.11 (s, 1H, NH). HPLC purity: t_R = 9.34, 100%. MS(ESI) m/z Calcd for $C_{17}H_{21}N_2O$ $[M + H]^+$ 269.1 found 269.1. Anal. Calcd. for $C_{17}H_{20}N_2O$: C, 76.09; H, 7.51; N, 10.44. Found C, 76.01; H, 7.55; N, 10.35.

Analytical data for ***N*-ethyl-*N*-((7-methoxy-*9H*-carbazol-4-yl) methyl)ethanamine (4b)**: yellow solid, m.p. 97–99 °C. Yield 91%. IR (KBr, cm^{-1}): 3383, 2967, 2934, 1626, 1577, 1497, 1314, 1289, 1114, 993, 819, 808, 757, 729. ^1H NMR (300 MHz, DMSO-d_6): δ 1.03 (t, J = 7.0 Hz, 6H), 2.60 (q, J = 7.0 Hz, 4H), 3.84 (s, 3H), 4.02 (s, 2H), 6.78 (dd, J = 8.0 Hz, 2.4 Hz, 1H), 6.96 (d, J = 2.4 Hz, 1H), 7.12 (d, J = 7.5 Hz, 1H), 7.25 (t, J = 7.5 Hz, 8.0 Hz, 1H), 7.34 (d, J = 8.0 Hz, 1H), 8.08 (d, J = 8.0 Hz, 1H), 11.15 (s, 1H). HPLC purity: t_R = 9.09, 100%. HRMS (ESI) m/z Calcd for $C_{18}H_{21}N_2O$ $[M-H]^-$ 281.1652 found 281.1653.

Analytical data for ***N*-benzyl-1-(7-methoxy-*9H*-carbazol-4-yl) methanamine (4c)**: yellow solid, m.p. 111–113 °C. Yield 81%. IR (KBr, cm^{-1}): 3399, 2823, 1621, 1494, 1309, 1226, 1197, 1166, 940, 775, 760, 737, 698. ^1H NMR (300 MHz, DMSO-d_6): δ 3.83 (s, 3H), 3.85 (s, 2H), 4.18 (s, 2H), 6.75 (dd, J = 8.0 Hz, 2.4 Hz, 1H), 6.97 (d, J = 2.4 Hz, 1H), 7.14 (d, J = 7.2 Hz, 1H), 7.27 (t, J = 7.2 Hz, 8.0 Hz, 2H), 7.39–7.31 (m, 3H), 7.41 (d, J = 6.9 Hz, 2H), 7.85 (d, J = 8.0 Hz, 1H), 11.16 (s, 1H). HPLC purity: t_R = 8.04, 100%. HRMS (ESI) m/z Calcd for $C_{21}H_{19}N_2O$ $[M-H]^-$ 315.1496 found 315.1495.

4.1.12. General procedure for the synthesis of 3-chloro-N-isopropyl-N- [(7-methoxydibenzo[b,d]furan-1-yl)methyl]propanamide (16a) and 3-chloro-N-isopropyl-N- [(7-methoxy-9H-carbazol-4-yl) methyl]propanamide (**16b**)

To an ice-cooled solution of compound **2a** (0.67 g, 2.5 mmol) or **4a** (0.67 g, 2.5 mmol), pyridine (0.24 g, 3.0 mmol) in 30 mL of anhydrous CH_2Cl_2 was added chloroacetyl chloride (0.32 g, 2.8 mmol) dropwise. The resulting solution was stirred at room

temperature for 1 h, and then washed with saturated Na_2CO_3 aqueous solution (50 mL × 3) and saturated NaCl aqueous solution (50 mL × 3), respectively. The organic phase was dried with anhydrous Na_2SO_4 and concentrated to give crude product which was further purified by column chromatography (petro ether/EtOAc = 5:1) to give the desired product.

Analytical data for **16a**: yellow oil. Yield 92%. IR (KBr, cm^{-1}): 2958, 1632, 1584, 1437, 1282. ^1H NMR (500 MHz, $CDCl_3$): δ 1.18 (d, J = 7.50 Hz, 6H), 2.99–3.01 (m, 1H), 3.90 (s, 3H), 4.24 (s, 2H), 4.87 (s, 2H), 6.96 (dd, J = 10.0 Hz, 2 Hz, 1H), 7.10 (d, J = 2.0 Hz, 1H), 7.26 (d, J = 10.0 Hz, 1H), 7.32 (t, J = 10.0 Hz, 1H), 7.42 (d, J = 10.0 Hz, 1H), 7.89 (d, J = 10.0 Hz, 1H). MS(ESI) m/z Calcd for $C_{19}H_{21}ClNO_3$ $[M + H]^+$ 346.1 found 346.1.

Analytical data for **16b**: pale yellow solid, m.p. 119–121 °C. Yield 90%. IR (KBr, cm^{-1}): 3394, 3280, 2977, 1732, 1647, 1497, 1437, 1306, 1198, 1159, 1119, 1034, 824, 802, 758, 731. ^1H NMR (300 MHz, DMSO-d_6): δ 1.17 (d, J = 6.9 Hz, 6H), 3.06–3.08 (m, 1H), 3.86 (s, 3H), 4.11 (s, 2H), 4.96 (s, 2H), 6.80 (dd, J = 8.65 Hz, 2.35 Hz, 1H), 7.02 (d, J = 2.25 Hz, 1H), 7.19 (d, J = 7.15 Hz, 1H), 7.25 (t, J = 7.35 Hz, 7.9 Hz, 1H), 7.37 (d, J = 8.05 Hz, 1H), 8.03 (d, J = 8.65 Hz, 1H), 11.32 (s, 1H). MS(ESI) m/z Calcd for $C_{19}H_{22}ClN_2O_2$ $[M + H]^+$ 345.1 found 345.1.

4.1.13. General procedure for the synthesis of N-isopropyl-N-[(7-methoxydibenzo[b,d]furan-1-yl)methyl]-3-nitropropanamide (3) and N-isopropyl-N-[(7-methoxy-9H-carbazol-4-yl)methyl]- 3-nitropropanamide (**5**)

A mixture of compound **16a** (0.69 g, 2.0 mmol) or **16b** (0.69 g, 2.0 mmol), silver nitrate (1.7 g, 10.0 mmol) in 50 mL of anhydrous acetonitrile was refluxed in the dark for 24 h. After cooling to room temperature, the deposit was filtrated off and the filtrate was concentrated under reduced pressure to give crude product which was further purified by column chromatography (petro ether/EtOAc = 5:1) to give the desired product.

Analytical data for **3**: yellow oil. Yield 54%. IR (KBr, cm^{-1}): 2988, 2847, 1648, 1579, 1484, 1503, 1282, 848. ^1H NMR (500 MHz, DMSO-d_6): δ 1.20 (d, J = 8.0 Hz, 6H, $CH(C\underline{H}_3)_2$), 2.82 (t, J = 8 Hz, 2H, $COC\underline{H}_2CH_2$), 3.02–3.05 (m, 1H, $C\underline{H}(CH_3)_2$), 3.74 (s, 3H, $OC\underline{H}_3$), 4.43 (s, 2H, $C\underline{H}_2NCH$), 4.98 (t, J = 8 Hz, 2H, $C\underline{H}_2ONO_2$), 6.55 (dd, J = 8.0 Hz, 2.5 Hz, 1H, arom), 6.67 (d, J = 2.5 Hz, 1H), 6.88 (d, J = 8.0 Hz, 1H, arom), 6.97 (d, J = 2.5 Hz, 1H, arom), 7.22–7.24 (m, 1H, arom), 7.32 (d, J = 8.0 Hz, 1H, arom). ^{13}C NMR (500 MHz, DMSO-d_6): δ 21.5, 33.2, 44.9, 47.0, 53.0, 62.0, 100.1, 115.5, 120.0, 122.8, 123.0, 123.8, 124.2, 125.1, 130.4, 157.9, 159.6, 164.2, 186.4. HPLC purity: t_R = 3.69, 99.87%. HRMS (ESI) m/z Calcd for $C_{20}H_{23}N_2O_6$ $[M + H]^+$ 387.1556 found 387.1556. Anal. Calcd. for $C_{20}H_{22}N_2O_6$: C, 62.17; H, 5.74; N, 7.25. Found C, 62.01; H, 5.65; N, 7.35.

Analytical data for **5**: yellow oil. Yield 43%. IR (KBr, cm^{-1}): 3317, 2921, 2850, 1641, 1610, 1498, 1454, 1307, 1282, 1198, 851, 805, 753, 726. ^1H NMR (500 MHz, DMSO-d_6): δ 1.13 (d, J = 6.5 Hz, 6H, $CH(C\underline{H}_3)_2$), 2.80 (t, J = 8 Hz, 2H, $COC\underline{H}_2CH_2$), 3.05–3.07 (m, 1H, $C\underline{H}(CH_3)_2$), 3.86 (s, 3H, $OC\underline{H}_3$), 4.22 (s, 2H, $C\underline{H}_2NCH$), 5.08 (t, J = 8 Hz, 2H, $C\underline{H}_2ONO_2$), 6.86 (dd, J = 8.0 Hz, 2.5 Hz, 1H, arom), 6.99 (d, J = 2.5 Hz, 1H, arom), 7.15 (d, J = 7.2 Hz, 1H, arom), 7.22 (t, J = 8.0 Hz, 7.2 Hz, 1H, arom), 7.33 (d, J = 8.0 Hz, 1H, arom), 7.99 (d, J = 8.0 Hz, 1H, arom), 11.28 (s, 1H, $N\underline{H}$). ^{13}C NMR (500 MHz, DMSO-d_6): δ 20.3, 35.8, 43.5, 44.8, 55.1, 62.0, 98.7, 108.0, 111.4, 119.0, 120.5, 121.5, 123.9, 125.0, 125.1, 137.8, 150.5, 155.8, 178.9. HPLC purity: t_R = 11.93, 98.62%. HRMS (ESI) m/z Calcd for $C_{20}H_{24}N_3O_5$ $[M + H]^+$ 386.1716 found 386.1713. Anal. Calcd. for $C_{20}H_{23}N_3O_5$: C, 62.33; H, 6.01; N, 10.90. Found C, 62.31; H, 6.95; N, 10.77.

4.1.14. General procedure for the synthesis of 9-[(isopropylamino) methyl]dibenzo[b,d]furan-3-ol (2f) and 5-[(isopropylamino) methyl]-9H-carbazol-2-ol (**4d**)

A solution of **2a** (0.27 g, 1 mmol) or **4a** (0.27 g, 1 mmol) disolved in 30 mL of 48% HBr aqueous solution was stirred and refluxed for 3 h, and then basified by 10% NaOH aqueous solution to pH = 8. The resulted solution was extracted with AcOEt (100 mL × 3). The organic phase was dried with anhydrous Na_2SO_4, and the solvent was removed under vacuum to give the crude product which was furtehr purified by column chromatography (petro ether/EtOAc = 10:1) to give the desired product.

Analytical data for **2f**: yellow oil. Yield 65%. IR (KBr, cm^{-1}): 3384, 2958, 1630, 1585, 1415, 1279, 1177, 874, 750, 715. ^1H NMR (300 MHz, DMSO-d_6): δ 1.16 (d, J = 7.5 Hz, 6H), 3.02–3.04 (m, 1H), 4.24 (s, 2H), 6.89 (dd, J = 7.5 Hz, 2.5 Hz, 1H), 7.08 (d, J = 2.5 Hz, 1H), 7.24 (d, J = 7.5 Hz, 1H), 7.31 (t, J = 8.0 Hz, 7.5 Hz, 1H), 7.45 (d, J = 8.0 Hz, 1H), 7.88 (d, J = 7.5 Hz, 1H). HPLC purity: t_R = 7.56, 98.67%. HRMS (ESI) m/z Calcd for $C_{16}H_{18}NO_2$ $[M + H]^+$ 256.1338 found 256.1336.

Analytical data for **4d**: yellow solid. Yield 71%. m.p. 111–112 °C. IR (KBr, cm^{-1}): 3398, 3273, 2966, 1626, 1580, 1437, 1374, 1235, 1171, 824, 803, 752, 727. ^1H NMR (500 MHz, DMSO-d_6): δ 1.12 (d, J = 6.3 Hz, 6H), 2.97–2.93 (m, 1H), 3.17 (s, 1H), 4.20 (s, 2H), 6.66 (dd, J = 8.4 Hz, 2.4 Hz, 1H), 6.82 (d, J = 2.4 Hz, 1H), 7.09 (d, J = 6.9 Hz, 1H), 7.22 (t, J = 6.9 Hz, 8.4 Hz, 1H), 7.28 (d, J = 7.8 Hz, 1H), 7.86 (d, J = 7.8 Hz, 1H), 9.39 (s, 1H), 10.99 (s, 1H). HPLC purity: t_R = 7.69, 99.09%. HRMS (ESI) m/z Calcd for $C_{16}H_{17}N_2O$ $[M-H]^-$ 253.1379 found 373.1348.

4.2. Biological studies

4.2.1. Cholinesterase inhibition assay in vitro

The cholinesterase inhibitory activity of the target compounds was measured using Ellman's assay. AChE (E.C.3.1.1.7, Type VI-S, from Electric Eel) and BChE (E.C.3.1.1.8, from equine serum) were purchased from Sigma–Aldrich (Steinheim, Germany). DTNB (Ellman's reagent), ATC and BTC iodides were obtained from Fluka (Buchs, Switzerland). The assay was performed as described in the following procedure: stock solutions of the test compounds were prepared in ethanol, 100 μL of which gave a final concentration of 10^{-3} M when diluted to the final volume of 3.32 mL. The highest concentration of the test compounds applied in the assay was 10^{-4} M (10% EtOH in the stock solution did not influence enzyme activity). In order to obtain an inhibition curve, at least five different concentrations (normally 10^{-4}–10^{-9} M) of the test compound were measured at 25 °C at 412 nm, each concentration in triplicate. For buffer preparation, 1.36 g of potassium dihydrogen phosphate (10 mmol) were dissolved in 100 mL of water and adjusted with KOH to pH = 8.0 ± 0.1. Enzyme solutions were prepared to give 2.5 units mL^{-1} in 1.4 mL aliquots. Furthermore, 0.01 M DTNB solution, 0.075 M ATC and BTC solutions, respectively, were used. A cuvette containing 3.0 mL of phosphate buffer, 100 μL of the respective enzyme, and 100 μL of the test compound solution was allowed to stand for 5 min, then 100 μL of DTNB were added, and the reaction was started by addition of 20 μL of the substrate solution (ATC/BTC). The solution was mixed immediately, and exactly 2 min after substrate addition the absorption was measured. For the reference value, 100 μL of water replaced the test compound solution. For determining the blank value, additionally 100 μL of water replaced the enzyme solution. The inhibition curve was obtained by plotting the percentage enzyme activity (100% for the reference) vs. logarithm of test compound concentration.

4.2.2. In vitro nitric oxide release assay

In vitro nitric oxide release, upon incubation of the test compound (2.4 mL of 100 μM) with either i) phosphate buffer solution (PBS) at pH 7.4 and 37 °C for 24 h, ii) PBS at pH 7.4 and 37 °C to which 90 μL rat serum had been added, was determined by quantification of nitrite produced by the reaction of nitric oxide with oxygen and water using the Griess reaction. Nitric oxide release data were acquired for test compounds using the following

procedure. Phosphate buffer solution (PBS) was prepared by dissolving KH_2PO_4 (50 mM) and NaH_2PO_4 (50 mM) in distilled water. This solution was titrated to physiological pH (7.4) using 0.01 N sodium hydroxide. Griess reagent was prepared by dissolving sulfanilamide (4.0 g) and N-naphtylenediamine dihydrochloride (0.2 g) in a mixture of 85% H_3PO_4 (10 mL) and distilled water (approximately 90 mL). An aliquot of 2.4 mL of a 5% dimethyl sulfoxide (DMSO) solution in PBS (10 mL of dimethyl sulfoxide and 190 mL of PBS) was used as blank control solution, which was maintained at 37 °C for 1 h with gentle shaking. Griess reagent (0.8 mL) was then added, and the mixture was maintained at 37 °C for 30 min with gentle shaking. A standard nitrite concentration-absorbance plot was prepared by dissolving $NaNO_2$ (0.1 mM) in blank solution, and an aliquot of this solution (2.4 mL) was maintained at 37 °C for 1 h with gentle shaking. Griess reagent (0.8 mL) was then added and the mixture was maintained for 30 min at 37 °C with gentle shaking. After incubation, this solution was further diluted by mixing different aliquots with variable volumes of dilution solvent (32 mL of Griess reagent and 96 mL of blank solution). These concentrations of $NaNO_2$ were used to plot a calibration curve from which the nitrite concentration for each test compound was calculated (±SEM, $n = 3$). The percentage nitric oxide released from the test compounds was determined by preparing 0.2 mM solutions in DMSO. An aliquot (0.12 mL) was diluted with PBS solution, and then rat serum (90 mL) was added. This solution was maintained at 37 °C for 1 h with gentle shaking, Griess reagent (0.8 mL) was added, and the mixture was maintained for 30 min at 37 °C with gentle shaking. The ultraviolet absorbance values for the control blank solution, calibration curve, and the test compounds were measured at 540 nm. The absorbance value for each test compound was corrected by subtracting the averaged blank control absorbance. The nitrite concentration was determined from the standard nitrite concentration-absorbance curve, which in turn was used to calculate the percentage of nitric oxide released from each test compound.

4.2.3. ThT fluorescence assay

Aβ42 (Chinapeptides Co., Ltd) was dissolved in DMSO to make a 200 μM stock solution. The stock solution was centrifuged at the speed of 12,000 rpm for10 min. The above supernatant was used for experiments. The tested compounds were dissolved in DMSO at concentrations of 0.2, 2.0, 4.0 mM. A screening assay for tested compounds to inhibit Aβ aggregation was performed by measuring ThT fluorescence emission. Each compound (in concentrations of 0.2–4.0 mM) (2 μL) and 2 μL of 200 μM Aβ42 were added into 76 μL of phosphate-buffered saline (PBS at pH 7.4) in a 96-well plate. After incubation for 1 h at room temperature, 80 μL of 5 μM ThT solution (in 50 mM glycine-NaOH at pH 8.5) was added to the reaction solution. Fluorescence emission was measured at 488 nm with an excitation wavelength of 430 nm on a multilevel HTS counter.

4.2.4. Atomic force microscopy

The tested compound (2.5 μL) (1.0 mM) and 2.5 μL of 200 μM Aβ42 were added to 45 μL of PBS buffer (20% TFE at pH 7.4). As a control, 2.5 μL of 200 μM Aβ42 was added to 47.5 μL of PBS buffer (20% TFE at pH 7.4). Samples were incubated at 37 °C for 6 days, and a 3 μL sample solution was deposited on freshly cleaved mica and incubated for 5 min, then blown dry. Amyloid formation was visualized with Molecular Imaging Picoplus II workstation (Molecular Imaging Corp.). AFM probe was NSC35-type from Molecular Imaging Corp. with resonant frequency of 170 kHz. The spring constant of the cantilever having the AFM tip was 45 N/m.

4.2.5. Cell viability analysis

PC12 cells, obtained from the Cell Bank of the Chinese Academy of Sciences (Shanghai, China), were cultured in a humidified, 5% CO_2 atmosphere at 37 °C, and maintained in monolayer culture in F-12 medium supplemented with 10% fetal bovine serum (FBS), 100 mg/mL of streptomycin and 100 mg/mL of penicillin. The cell viability was determined by MTT assay (MTT: 3-(4,5-dimethylthiazol-2-yl)-2,5-diphenyltetrazolium bromide). For the preparation of Aβ42 solution, Aβ42 (Chinapeptides Co., Ltd) was initially dissolved to 1 mM in hexafluoroisopropanol (Sigma) and separated into aliquots in sterile microcentrifuge tubes. Hexafluoroisopropanol was removed under vacuum in a Speed Vac, and the peptide film was stored dessicated at −20 °C. F-12 culture medium was added to bring the peptide to a final concentration of 100 μM and incubated at 4 °C for 24 h. The tested compounds were dissolved in DMSO and diluted to the required concentration with culture medium (DMSO final concentration < 0.5%). The suspension of 2000 cells/well was plated in 96-well culture plates with culture medium and was incubated for 24 h at 37 °C, in a 5% CO_2 incubator. Then 24 μL of tested compound solution (final concentrations ranging between 0.008 μM and 10 μM), or 24 μL of tested compound solution (final concentrations ranging between 0.008 μM and 10 μM) containing Aβ42 (final concentration 5 μM) was added. Cells were incubated at 37 °C for 24 h. respectively. After that, the cells were treated with 10 mL MTT dye solution (5 mg/mL) for 4 h cultivation. The media with MTT solution were removed with 100 mL of DMSO solution. The absorbance of formazane solution was measured at 540 nm with an automatic microplate ELISA reader. Wells without cells were used as blanks and were subtracted as background from each sample. Results were expressed as a percentage of control. Three independent trials were analyzed and the results were expressed as mean ± SEM.

4.2.6. Behavioral studies

Investigations were performed on 60-day-old female Wistar rats (Han:Wist) of the out-bred stock of the Institute of Pharmacology and Toxicology, Jena University Hospital, Germany. Rats were housed in a room that was automatically maintained on a 12-h light/dark cycle at 25 °C and proper humidity. Rats were given food (Altromin 1326®, Altromin, Lage, Germany) and tap water ad libitum. The permission of the animal protection commission of the State of Thuringia, Germany, was given. Scopolamine hydrobromide trihydrate was obtained from Sigma Chemicals, Munich, Germany. 0.05 mg/100 g b. wt. were dissolved in saline and administered intraperitoneally (i. p.) 5 min after tacrine or the test compounds, respectively. Tacrine hydrochloride (BioTrend Wangen/Zürich, Switzerland) was dissolved in phosphate buffer (pH 7.4) and 0.24 mg/100 g b. wt., corresponding to 1.0 μmol/100 g b. wt., were administered i. p. The new substances were dissolved in saline.

We examined whether the new compounds could improve spatial memory impairment induced by scopolamine using RAM performance. Each arm (44 cm L, 30 cm H, 14 cm W) radiated from an octagonal platform that served as a starting point. A food cup (3 cm diameter) was located at the end of each arm. The entire arms and food cups were painted gray and placed in a dark and calm room. Animal behavior was monitored by a video camera. Image analysis and pattern recognition from the monitor were performed by a VideoMot 2 program (video tracking, motion analysis, and behavior recognition system) provided by TSE Systems (Bad Homburg, Germany). The computerized recording systems were located in the same room.

Two phases of pre-training were performed: After a short handling period (phase 1) in which the rats were in close contact with the laboratory staff, three rats experienced free movement

and feeding in the RAM once a day for 5 days to adapt to the maze and bait (phase 2 = adaptation). The baits were scattered in all arms. After handling and adaptation of the rats to the maze, food was restricted to reduce the rat's body weight by 10%. Then the training trial was started. Each rat was placed once daily in the centre of the RAM to visit all eight arms and eat all reward food baits (Dustless precision Rodent Pellets, Bilaney Consultants Ltd., Sevenoaks, Kent, U.K.) in each food cup. Each trial was performed until the rat entered and ate all the pellets in the eight arms. Rats were trained to a criterion of trials without error in less than 60 s at three consecutive days. Then the experiments started. The rats that did not reach this standard were eliminated from the study.

One day after the training trials the experiments were carried out. Before the administration of a substance a control run was performed. Thus, each animal was its own control. Thereafter cognition impairment was induced by administration of scopolamine. Tacrine or the new compounds were given i. p. 5 min before scopolamine. The following parameters were registered at different times after scopolamine:

- time needed to visit all arms (total searching time)
- errors (re-entry into an arm that has been previously visited)
- the number of the baits not found after 10 min

The trial was finished either the rat had eaten all pellets or 10 min were elapsed or 16 errors were done. The maze test was carried out before and 20, 60, and 120 min after scopolamine administration.

4.2.7. Biochemical investigations ex vivo

For the determination of the tissue content of lipidperoxidation products as thiobarbituric acid reactive substances, organ samples were homogenized with 19 volumes of ice cold saline and the analysis was carried out fluorometrically. Tissue content of reduced and oxidized glutathione (GSH; GSSG) was determined according to following precedures, respectively: samples were homogenized with 11 volumes of 0.2 M sodium phosphate buffer (5 mM EDTA; pH 8.0) and 4 volumes of 25% metaphosphoric acid. After centrifugation (12 000× g; 4 °C, 30 min) GSH and GSSG were measured in the supernatants photometrically or fluorometrically, respectively.

Liver biotransformation capacity was assessed in liver tissue 9000× g supernatants by measuring three model reactions for different cytochrome P450 isoforms: ethoxyresorufin-O-deethylation (ErOD; CYP1A1 and 1A2), ethoxycoumarin-O-deethylation (EcOD; CYP1A, 2A, 2B, 2C), and ethylmorphine-N-demethylation (END; CYP3A). For preparation of 9000× g supernatants liver specimens were homogenized in 0.1 M sodium phosphate buffer pH 7.4 (1:3 w/v) and the homogenate was centrifuged at 9000× g at 4 °C for 20 min. The protein content of the supernatants was determined with the Biuret method. Ethoxyresorufin-O-deethylation was measured according to Pohl and Fouts [29], fluorometrically determining the metabolite resorufin. With ethoxycoumarin-O-deethylation the main metabolite 7-hydroxycoumarin was assessed fluorometrically. Ethylmorphine-N-demethylation was performed according to Klinger and Müller [30], determining the reaction product formaldehyde photometrically. The activities of the model reactions were referred to the protein content of the 9000× g supernatants.

The number of animals investigated per group for the histological and biochemical investigations comprised $n = 6$. The results of the clinical chemistry analyses and of the biochemical experiments are expressed as arithmetic means S.E.M. For statistical analysis Student's t-test ($p < 0.05$) was applied.

Acknowledgments

This work is supported by National Natural Science Foundation of China (No. 81001361), the New Drug Creation Project of the National Science and Technology Major Foundation of China (Project 2013ZX09402102-001-006), Ph.D. Programs Foundation of Ministry of Education of China (No. 20100092120046) and the Open Project Program of State Key Laboratory of Natural Medicines, China Pharmaceutical University. Dr. Fang is grateful to the support of Alexander von Humboldt Foundation.

Appendix A. Supplementary data

Supplementary data related to this article can be found at http://dx.doi.org/10.1016/j.ejmech.2014.02.035.

References

[1] H.W. Querfurth, F.M. LaFerla, The New England Journal of Medicine 362 (2010) 329–344.
[2] R. Jakob-Roetne, H. Jacobsen, Angewandte Chemie International Edition 48 (2009) 3030–3059.
[3] J.L. Cummings, H.V. Vinters, G.M. Cole, Z.S. Khachaturian, Neurology 51 (1998) S2–S17.
[4] C. Geula, Neurology 51 (1998) S18–S29.
[5] W. Yang, Y. Wong, O.T.W. Ng, L.P. Bai, D.W.J. Kwong, Y. Ke, Z.H. Jiang, H.W. Li, K.K.L. Yung, M.S. Wong, Angewandte Chemie International Edition 51 (2012) 1804–1810.
[6] A.K. Sharma, S.T. Pavlova, J. Kim, D. Finkelstein, N.J. Hawco, N.P. Rath, J. Kim, L.M. Mirica, Journal of the American Chemical Society 134 (2012) 6625–6636.
[7] A. Cavalli, M.L. Bolognesi, A. Minarini, M. Rosini, V. Tumiatti, M. Recanatini, C. Melchiorre, Journal of Medicinal Chemistry 51 (2008) 347–372.
[8] J. Marco-Contelles, M. do Carmo Carreiras, C. Rodríguez, M. Villarroya, A.G. García, Chemical Reviews 106 (2006) 116–133.
[9] C. Guillou, A. Mary, D.Z. Renko, E. Gras, C. Thal, Bioorganic & Medicinal Chemistry Letters 10 (2000) 637–639.
[10] S. Berkov, C. Codina, F. Viladomat, J. Bastida, Bioorganic & Medicinal Chemistry Letters 18 (2008) 2263–2266.
[11] P. Jia, R. Sheng, J. Zhang, L. Fang, Q. He, B. Yang, Y. Hu, European Journal of Medicinal Chemistry 44 (2009) 772–784.
[12] E. Simoni, S. Daniele, G. Bottegoni, D. Pizzirani, M.L. Trincavelli, L. Goldoni, G. Tarozzo, A. Reggiani, C. Martini, D. Piomelli, C. Melchiorre, M. Rosini, A. Cavalli, Journal of Medicinal Chemistry 55 (2012) 9708–9721.
[13] L. Vezenkov, J. Sevalle, D. Danalev, T. Ivanov, A. Bakalova, M. Georgieva, F. Checler, Current Alzheimer Research 9 (2012) 600–605.
[14] A.H. Lewin, J. Szewczyk, J.W. Wilson, F.I. Carroll, Tetrahedron 61 (2005) 7144–7152.
[15] P. Keglevich, P. Kovacs, L. Hazai, Z. Santa, Z. Dubrovay, V. Hada, C.J. Szantay, G. Kalaus, C. Szantay, Heterocycles 84 (2012) 1171–1178.
[16] H.M. Greenblatt, G. Kryger, T. Lewis, I. Silman, J.L. Sussman, FEBS Lett 463 (1999) 321–326.
[17] G.R.J. Thatcher, B.M. Bennett, J.N. Reynolds, Current Alzheimer Research 2 (2005) 171–182.
[18] L. Fang, D. Appenroth, M. Decker, M. Kiehntopf, C. Roegler, T. Deufel, C. Fleck, S. Peng, Y. Zhang, J. Lehmann, Journal of Medicinal Chemistry 51 (2008) 713–716.
[19] L. Fang, D. Appenroth, M. Decker, M. Kiehntopf, A. Lupp, S. Peng, C. Fleck, Y. Zhang, J. Lehmann, Journal of Medicinal Chemistry 51 (2008) 7666–7669.
[20] F.W. Wassmundt, R.P. Pedemonte, The Journal of Organic Chemistry 60 (1996) 4991–4994.
[21] A.W. Freeman, M. Urvoy, M.E. Criswell, The Journal of Organic Chemistry 70 (2005) 5014–5019.
[22] P.G. Wang, M. Xian, X. Tang, X. Wu, Z. Wen, T. Cai, A.J. Janczuk, Chemical Reviews 102 (2002) 1091–1134.
[23] S. Rizzo, A. Bisi, M. Bartolini, F. Mancini, F. Belluti, S. Gobbi, V. Andrisano, A. Rampa, European Journal of Medicinal Chemistry 46 (2011) 4336–4343.
[24] L.C. Lopez, S. Dos-Reis, A. Espargaro, J.A. Carrodeguas, M.L. Maddelein, S. Ventura, J. Sancho, Journal of Medicinal Chemistry 55 (2012) 9521–9530.
[25] K.N. Dahlgren, A.M. Manelli, W.B. Stine Jr., L.K. Baker, G.A. Krafft, M.J. LaDu, The Journal of Biological Chemistry 277 (2002) 32046–33253.
[26] C. Dezfulian, A. Alekseyenko, K.R. Dave, A.P. Raval, R. Do, F. Kim, M.A. Perez-Pinzon, Nitric Oxide 26 (2012) 241–250.
[27] I.T. Schiefer, L. VandeVrede, M. Fa', O. Arancio, G.R. Thatcher, Journal of Medicinal Chemistry 55 (2012) 3076–3087.
[28] B.A. Wirsching, R.J. Benninger, K. Jhamandas, R.J. Boegman, S. El-Defray, Pharmacology Biochemistry and Behavior 20 (1984) 659–662.
[29] R.J. Pohl, J.R. Fouts, Analytical Biochemistry 107 (1980) 150–155.
[30] W. Klinger, D. Müller, Acta Biologica et Medica Germanica 36 (1977) 1149–1159.